Time Scales for SST over the Global Ocean

C. N. Barron and A. B. Kara

Oceanography Division, Naval Research Laboratory, Stennis Space Center, Mississippi, USA

C. L. Gentemann

Remote Sensing Systems, Santa Rosa California, USA

W.–Y. Loh

Department of Statistics, University of Wisconsin, Madison, WI, USA

A. Birol Kara, Naval Research Laboratory, Oceanography Division, Code 7320, Bldg. 1009, Stennis Space Center, MS 39529, USA. (Birol.Kara@nrlssc.navy.mil)

Abstract. Time scales of sea surface temperatures (SST) are examined using three daily products over the global ocean from June 2002 through June 2006. These SST show good agreement overall, demonstrating high skill over most of the global ocean. Some differences among them are evident in the tropical regions and particularly in the western equatorial Pacific warm pool. Auto–correlation values computed using daily time series from each product give similar patterns over the global ocean. The resulting lags from each daily SST product give typical values of < 10 days in the inter-tropical convergence zone, > 30 days in mid–latitudes and $20-30$ days in the high latitudes. Regions of longer lags in broad areas of the southern hemisphere and shorter time scales in the vicinity of major frontal boundaries reveal consistent inter–annual variability across all three products.

1. Introduction

Time scales of SST variability reflect feedbacks and balances among the factors that regulate heat budgets over the global ocean. These factors are distinctly different between tropical regions and mid–latitudes. For example, *Seager et al.* [1988] explains that away from the equatorial regions, SST is primarily determined by a one–dimensional balance of heat storage in the ocean mixed layer, resulting in a simple annual cycle of temperature. *Carton et al.* [1996] provide similar findings. The net heat flux is also the main contributor for SST variability of the ocean in mid–latitudes [*Cayan*, 1992].

Some penetrating solar energy is normally trapped within and below the seasonal pycnocline in mid–latitudes where large seasonal variations in mixed layer depth occur [e.g., *Kara et al.*, 2004]. In equatorial regions, however, solar energy normally does not penetrate below the mixed layer depth and thus is used entirely to heat the mixed layer. Different processes may be regionally dominant: extensive cloudiness and precipitation in low latitudes under the influence of the Inter-tropical Convergence Zone (ITCZ) [*Yuter and Houze*, 2000], effects of stratocumulus clouds in cooler areas of eastern tropics [*Bretherton et al.*, 2004], and upwelling or fog banks along coastal regions.

Discussions above reveal various time scale dependancies for SST regionally. For instance, SST timescales vary from 1 week to 45 days in the Sicily Channel of the Mediterranean Sea [*Borzelli and Ligi*, 1999]. Similarly, decorrelation time scales for SST were found to be from 2 to 6 days in the California Current region [*Abbott and Letelier*, 1988]. A study that quantifies the time scales for SST has not been established over the global ocean, which we will investigate in this paper.

2. SST Products and Evaluations

We use daily SSTs from three products: the 1/8° infrared (IR) Modular Ocean Data Assimilation System (MODAS) SST analysis from the Naval Research Laboratory [*Barron and Kara*, 2006], the 1/4° microwave (MW) SST from Remote Sensing Systems (RSS) [*Gentemann et al.*, 2004], and the 1/2° blended IR and in situ Real–Time Global (RTG) SST analysis from the National Centers for Environmental Prediction (NCEP) [*Thiébaux et al.*, 2003].

Major attributes of each product may be compared in Table 1. All use separate implementations of optimum interpolation to fill voids and blend data into daily global SST on relatively fine global grids, calibrated to represent bulk temperature. Each constructs fields using different error covariances, with shorter length scales in MODAS to preserve details and longer length scales in RTG to smooth over irregularities or missing data. All begin with the prior analysis as a first guess, but MODAS and RTG additionally adjust these toward climatology. All rely on satellite observations, but over different wavelengths; MODAS and RTG use infrared while RSS uses microwave.

MODAS and RTG utilize Advanced Very–High Resolution Radiometer (AVHRR) retrievals from NOAA polar–orbiting satellites. The data have spatial resolution of about 4 km. These IR observations are obscured by cloud cover, leading to reduced accuracy under persistently cloudy conditions. RTG additionally incorporates in situ observations, which can locally mitigate the cloud-induced data voids. *Kara and Barron* [2007] found that the high spatial resolution is an advantage for MODAS in improving patterns of daily

SSTs, while including in situ SSTs is an advantage for RTG, especially in the equatorial Pacific warm pool.

Microwave–based SSTs from RSS are derived from the Tropical Rainfall Measuring Mission (TRMM) Microwave Imager (TMI) [*Kummerow et al.*, 1998] and the Advanced Microwave Scanning Radiometers for Earth Observing Systems EOS (AMSR–E). TRMM's high–inclination orbit limits data to 40°S–40°N, while AMSR–E retrieves SST globally. A key advantage of microwave SST is its ability to make retrievals through cloud cover. Both TMI and AMSR–E SSTs are disadvantaged by the lower spatial resolution (25 km) and loss of useful retrievals within 50 km of land.

Given these differences in the SST products, we would like to examine their relative characteristics before proceeding to additional applications. Inter–comparisons among SST products are performed over the entire global ocean during 1 June 2002–1 June 2006, a time period which is common for all products. SSTs from MODAS, RSS and RTG are first interpolated to a common grid of 1/8° before performing inter–comparisons. Two statistical metrics, mean bias and skill score, are then computed based on daily time series at each grid point.

The mean bias is simply the average SST difference between two products. SST skill score includes two non–dimensional biases (the bias due to mean and the bias due to standard deviation between two products), and accounts for a linear correlation coefficient [*Murphy* 1995]. It is computed as $1 - \mathrm{RMS}^2/\mathrm{std}^2$, where RMS is the root–mean–square SST difference between the two products and std is standard deviation of the SST time series of the reference product. Skill score can therefore serve as a non–dimensional metric over the global ocean. A skill value of 1.0 indicates that SSTs from two products are identical, i.e., they agree perfectly well, while negative skill values indicate poor agreement.

Mean bias and skill score are presented during the common time period (Figure 1). Computations are performed between the pairs of RSS versus MODAS, RTG versus MODAS, and RTG versus RSS. While SST biases are found in some regions, global averages are close to zero (Figure 1a). The mean biases (i.e., RSS–MODAS) show that SSTs from RSS are slightly colder than those from MODAS in the tropical Pacific, northern Indian Ocean, and high southern latitudes. Such biases typically disappear except at the high southern latitudes when comparing RTG with MODAS.

SSTs from RTG are warmer in the northern Atlantic and Pacific Oceans than either RSS or MODAS. Biases (RTG–MODAS) can exceed 0.4°C. Similar warm bias between RTG and RSS extends into the eastern equatorial Pacific and Indian Ocean; RTG and MODAS are in better agreement in these areas. Some smaller-scale bias patterns between RSS versus MODAS and RTG vs MODAS within the Gulf Stream region appear to be a consequence of the higher resolution spatial scales in MODAS, as these patterns are almost absent in comparisons of the two coarser resolution products. All products generally reveal some differences in zones of coastal upwelling and the offshore extension of western boundary currents.

Overall agreement among all SST products is reflected in the skill scores, which are close to a perfect value of 1 over a majority of the global ocean. Areas of no skill at very high latitudes likely indicate differences in representing the ice edge. SST skill, generally low in the ITCZ, becomes negative between the pairs of RSS versus MODAS and RTG versus

RSS in the western equatorial Pacific and near the northwestern Indian Ocean. RTG versus MODAS shows no areas of negative skill but does indicate lower skill in the ITCZ. Persistent cloudiness in these low latitudes and observations on different spatial scales contribute to the low skill scores between the RSS product based on cloud–penetrating microwave retrievals and the infrared–based RTG and MODAS products. Relatively low SST standard deviation in low latitude areas amplifies the impact of SST differences, leading to reduced skill score.

3. Time Scales for SST Dependence

We use daily SSTs from MODAS, RTG and RSS to investigate SST time scales over the global ocean by calculating auto–correlation at each grid point. The auto–correlation is a correlation of a time series with itself over successive time intervals [e.g., *Phillips et al.*, 1999], computed by the sum of the cross products shifted by a variable lag. Auto–correlation reveals how SST for a given day tend to relate to SST on an earlier day. As an example, lag values based on an auto–correlation value of 0.7 are obtained from each SST product in 2005 (Figure 2). We take the value of 0.7 to indicate the maximum lag that still indicates a strong relationship. An auto–correlation of 0.7 at lag k implies that $\approx 50\%$ $(0.7 \times 0.7 = 0.49)$ of the variability of SST at day t can be explained by the SST at day $t - k$.

The time scale analysis reveals very similar lag values from MODAS, RTG and RSS over most of the global ocean. MODAS SSTs tend to have longer time correlation scales than RTG or RSS, especially in the western equatorial Pacific Ocean where cloudiness and exclusion of in situ observations cause MODAS SSTs to relax more strongly toward climatology. SST time scales are always shorter (typically < 10 days) in the tropical regions; RTG indicates the shortest time scales as the in situ SST incorporated to the analysis captures higher frequency variability. Time scales from RSS fall between RTG and MODAS, reflecting both more continuous, cloud–penetrating observations and longer spatial scales that may not resolve the finer spatial variations. Time scales are 3–4 times longer away from the equator and even exceed 50 days in some locations between 0° and 20°S off the coast of South America.

Finally, we investigate whether or not there are inter–annual variations in time scales for SST. Lag values for SST are calculated in the equatorial Pacific (Figure 3a) and in a region including the Gulf Stream current system (Figure 3b). Results are shown for each SST product in 2003, 2004 and 2005, separately. The overall patterns of SST time scales show little inter–annual variability, indicating robustness in these time scales. Inter–annual differences in time scales are more clearly evident in the equatorial Pacific, a consequence of the relatively larger span of temporal scales in the tropics. While changes are less clear in the Gulf Stream region, localized regions of shorter time scales do change, indicating areas of more significant variability in the Gulf Stream pathway or eddy activity.

4. Conclusions

SST time scales derived from three multi–year global SST time series reveal similar overall distributions. No significant inter–annual variability is found in the overall SST scales but changes can be identified locally. Our confidence in these findings is bolstered by the differences in the data sources and methodologies used in creating the SST products.

The robustness of the scales among different products and over different years indicates that these reflect persistent processes and balances.

In equatorial regions, short scales reflect episodic rain events and cloud–dominated variability in solar heating. Shorter time scales along the edges of western boundary currents and the Antarctic Circumpolar Current highlight areas of front variability. Narrow regions of short time scales indicate zones of coastal upwelling along eastern ocean boundaries such as the California coast. Longer time scales seem to correspond with regions of significant stratocumulus cloud cover examined by *Bretherton et al.* [2004]. Seasonal cycles are more important farther from the equator, leading to mid–range decorrelation lags on the order of a month over much of the ocean. The daily sampling of these products precludes consideration of diurnal variability; such consideration could utilize the RSS diurnal model and other products with diurnal resolution in a future study. This global view of SST time scales may help to define common properties and identify changes over longer time periods.

Acknowledgments.

The help of L. Smedstad is greatly acknowledged. This work is a contribution under the Multi-sensor Improved Sea Surface Temperature (MISST) for GODAE project. W.-Y. Loh's participation is supported by National Science Foundation grant, DMS-0402470. This paper is contribution NRL/JA/7320/320/08/8083 and has been approved for public release.

References

Abbott, M. R., and R. M. Letelier (1988), Decorrelation scales of chlorophyll as observed from bio–optical drifters in the California Current, *Deep Sea Res.*, Part II, *45*, 1639–1667.

Barron, C. N., and A. B. Kara (2006), Satellite–based daily SSTs over the global ocean, *Geophys. Res. Lett.*, *33*, L15603, doi:10.1029/2006GL026356.

Borzelli, G., and R. Ligi (1999), Auto–correlation scales of the SST distribution and water masses stratification in the Channel of Sicily, *J. Atmos. Oceanic Technol.*, *16*, 776–781.

Bretherton, C. S., T. Uttal, C. W. Fairall, S. E. Yuter, R. A. Weller, D. Baumgardner, K. Comstock, R. Wood, and G. B. Raga (2004), The EPIC 2001 stratocumulus study, *Bull. Amer. Met. Soc.*, *85*, 967–977.

Carton, J. A., X. Cao, B. S. Giese, and A. M. da Silva (1996), Decadal and interannual SST variability in the tropical Atlantic Ocean, *J. Phys. Oceanogr.*, *26*, 1165–1175.

Cayan, D. R. (1992), Latent and sensible heat flux anomalies over the northern oceans: Driving the sea surface temperature, *J. Phys. Oceanogr.*, *22*, 859–881.

Gentemann, C. L., F. J. Wentz, C. M. Mears, and D. K. Smith (2004), In–situ validation of Tropical Rainfall Measuring Mission microwave sea surface temperatures temperatures?, *J. Geophys. Res.*, *109*, C04021, doi:10.1029/2003JC002092.

Kara, A. B., H. E. Hurlburt, P. A. Rochford, and J. J. O'Brien (2004), The impact of water turbidity on the inter–annual sea surface temperature simulations in a layered global ocean model, *J. Phys. Oceanogr.*, *34*, 345–359.

Kara, A. B., and C. N. Barron (2007), Fine–resolution satellite–based daily sea surface temperatures over the global ocean, *J. Geophys. Res.*, *112*, C05041, doi:10.1029/2006JC004021.

Kummerow, C., W. Barnes, T. Kozu, J. Shieu, and J. Simpson (1998), The tropical rainfall measuring mission (TRMM) sensor package, *J. Atmos. and Oceanic Technol.*, *15*, 809–817.

Murphy, A. H. (1995), The coefficients of correlation and determination as measures of performance in forecast verification, *Wea. Forecasting*, *10*, 681–688.

Phillips, C. L., J. M. Parr, and E. A. Riskin (2002), *Signals, Systems, and Transforms*, 680 pp., Prentice Hall, New Jersey.

Seager, R., S. E. Zebiak, and M. A. Cane (1988), A model of the tropical Pacific sea surface temperature climatology, *J. Geophys. Res.*, *93*, 1265–1280.

Thiébaux, J., E. Rogers, W. Wang, and R. A. Houze Jr. (2000), A new high–resolution blended real–time global sea surface temperature analysis, *Bull. Amer. Met. Soc.*, *84*, 645–656.

Yuter, S. E., and B. Katz (2003), The 1997 Pan American Climate Studies Tropical Eastern Pacific Process Study. Part I: ITCZ Region, *Bull. Amer. Met. Soc.*, *81*, 451–481.

Table 1. Major Features of SST Products

Characteristics	MODAS	RSS	RTG
Resolution	1/8°	1/4°	1/2°
Time period	Jan 1993 onwards	Jun 2002–onwards	Feb 2001–onwards
Global domain	80°S–80°N	90°S–90°N	90°S–90°N
Availability	daily	daily	daily
Great Lakes	not included	included	included
Data collection	AVHRR	TMI, AMSR–E	AVHRR
Data collection	TIROS–N, NOAA–11,18	TRMM Aqua	NOAA–11, 16,17
Input SSTs	Infrared	Microwave	Infrared, in–situ
Length scale	20 km	100 km	100–450 km
SST type	bulk	bulk	bulk
SST on ice	no	no	yes
Missing data	none	near land	none
Ice mask	none	SSM/I ice mask	none
Diurnal model	none	exists	none
1st guess field	clim adjust prev day	previous day	clim adjust prev day
Distribution	www7320.nrlssc.navy.mil/modas2d	www.remss.com	polar.ncep.noaa.gov/sst

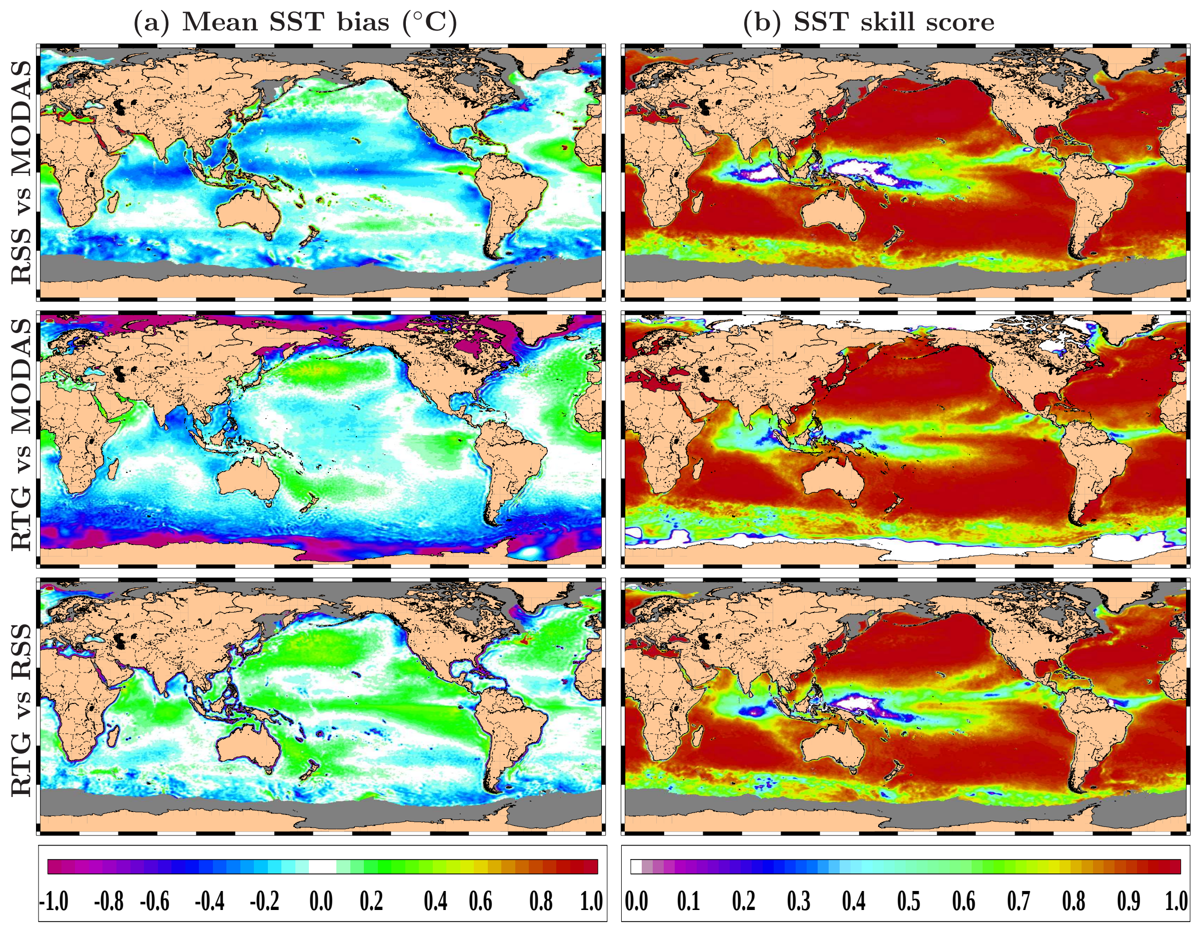

Figure 1. Mean bias and skill score between pairs of SST products over the global ocean. Computations are performed based on daily SST time series at each grid point during the 4–year time period from 1 June 2002 to 1 1 June 2006. A newer, 1/12° RTG running since September 2005 does not cover our analysis period so it is not used here. The regions where ice exists are shown by gray. Note that SSTs from RTG and MODAS are both available at the high latitudes where ice exists and thus mean biases are included in the map. However, MODAS does not have any specific treatment of SSTs in the existence of ice, and it just uses interpolated value from the nearest grid point.

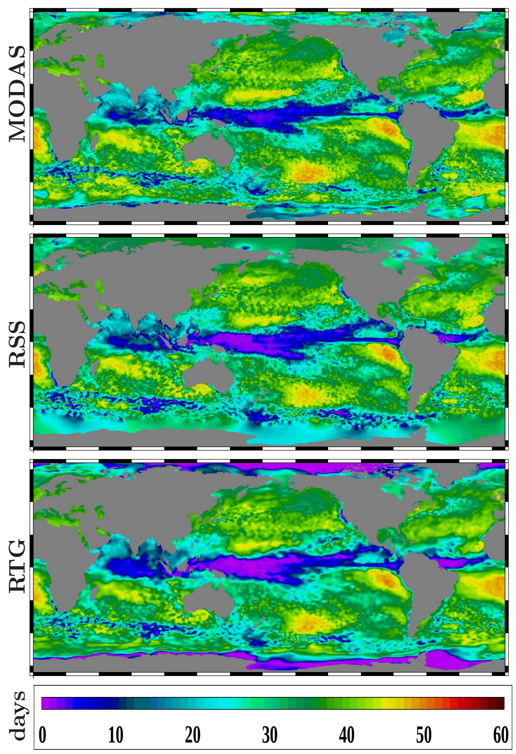

Figure 2. Lag values in days corresponding to an auto–correlation value of 0.7 for each SST product, which are computed using daily SST values in 2005 (i.e., January 1st–December 31st).

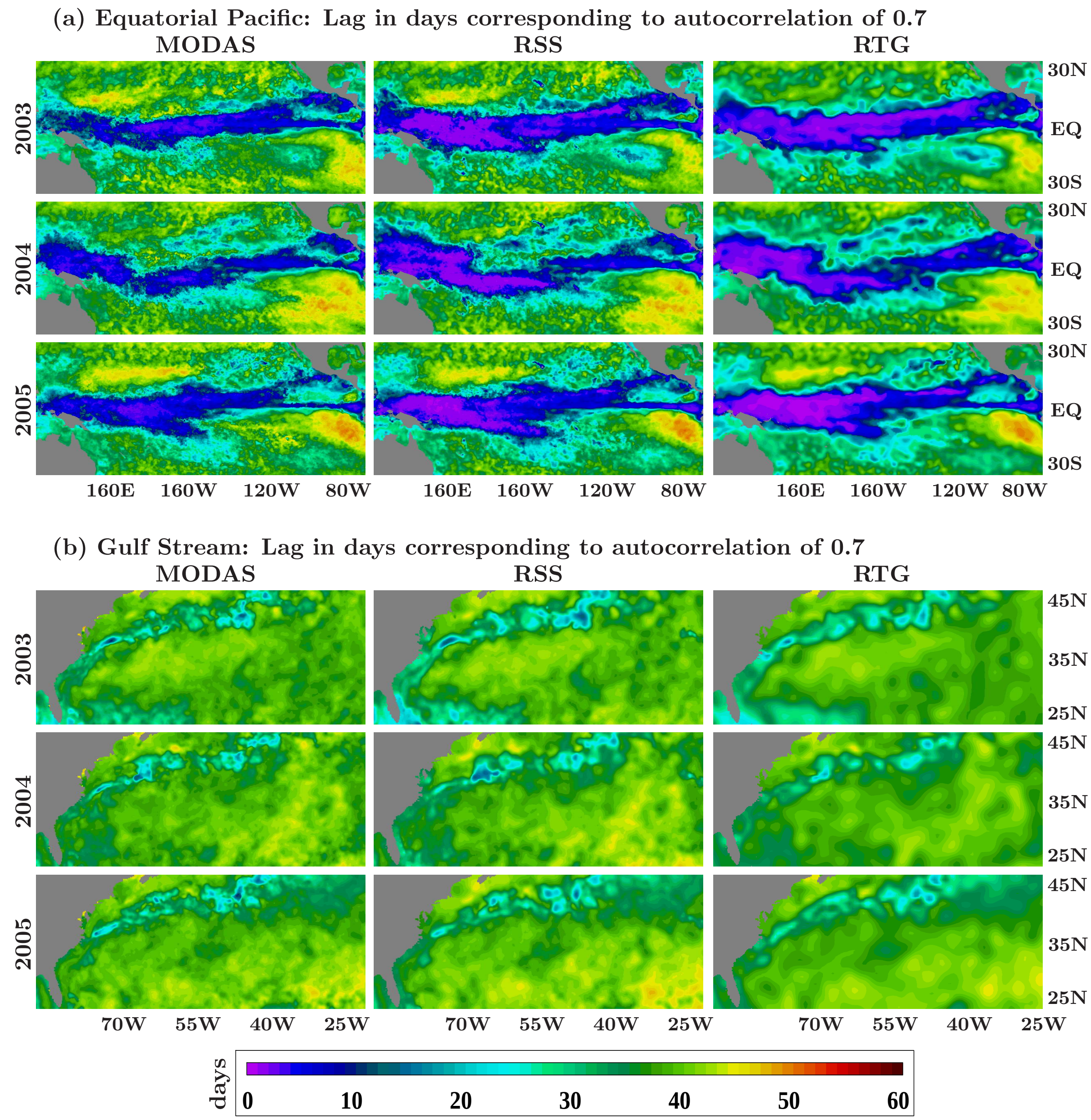

Figure 3. Lag values in days corresponding to an auto–correlation value of 0.7 in two regions: (a) The equatorial Pacific Ocean, spanning the latitudes from 30°S to 30°N, and (b) a region in the Atlantic Ocean including the Gulf Stream current system spanning the latitudes from 25°N to 45°N. Lags are calculated using daily SSTs (1 January through 31 December) from each product for each year of 2003, 2004 and 2005, separately.